Journal of Sound and Vibration (1997) **208**(4), 587–601

STABILITY CHARACTERISTICS OF SLENDER FLEXIBLE CYLINDERS IN AXIAL FLOW BY THE FINITE ELEMENT METHOD

C. P. VENDHAN AND S. K. BHATTACHARYYA

Ocean Engineering Centre, Indian Institute of Technology, Madras 600 036, *India*

AND

K. SUDARSAN

Naval Physical and Oceanographic Laboratory, Cochin 682021, *India*

(*Received* 17 *August* 1995, *and in final form* 26 *June* 1997)

The dynamics of flexible slender circular cylinders in axial flow having regard to their fluidelastic instability characteristics is an extensively studied problem in the literature. A finite element formulation of the problem is presented in this paper. The formulation has been validated with the analytical results of supported cylinders available in the literature. Additional numerical examples are presented for which analytical methods are difficult to formulate and do not exist in the literature, in order to bring out the breadth of application of the finite element method.

1. INTRODUCTION

The dynamics of flexible circular cylinders in axial flow has been studied extensively because such structures find use in many engineering applications [1, 2]. This class of problems exhibit fluidelastic instabilities of divergence and flutter. Though the mechanics of these problems is strongly non-linear both in hydrodynamic and structural dynamic aspects, these instabilities about any equilibrium position can be identified using linear approximation. The theoretical study of flexible cylinders in axial flow, in recent times, started in connection with the design of nuclear reactor cores to understand the dynamic behaviour of fuel rod bundles. Later it found important application in towing of cylindrical objects by ship for sonar as well as seismic applications.

Numerical modelling of this class of problems by the finite element method is attempted in this paper, presumably for the first time. This will enhance the capability to model real life structures which are not uniform in their geometry, inertial properties, stiffness as well as hydrodynamic properties over their lengths. Constant values of these properties are assumed in all available analytical methods. The finite element method can also treat practical structures consisting of multispan cylinders which are difficult to treat by analytical methods and therefore never attempted in the literature. The numerical results presented are firstly concerned with the validation of the finite element method using some of the examples documented in the literature and secondly with a few cases for which analytical solutions either do not exist or are difficult to obtain.

The fundamental formulation of the differential equation governing the dynamics of flexible slender cylinders under external axial flow, with several special effects included, is presented in references [3, 4]. Some later papers in this area [5–7] deal with various

0022–460X/97/490587 + 15 $25.00/0/sv971192

specialised aspects and approximations of the problem. In all these studies, the basic hydrodynamic models used had been based on the fundamental work reported in references [8, 9].

2. GOVERNING EQUATION

The differential equation governing small lateral motion of a uniform, flexible, slender circular cylinder in uniform axial flow (see Figure 1) can be written as [3, 4]

$$\mu I\dot{V}'''' + EIV'''' + (m+M)\ddot{V} + MU^2V'' + [(a_1 x - a_2)V'' + a_1 V'] + 2MU\dot{V}' + a_3 V' + a_4 \dot{V} = 0, \tag{1}$$

where

$$M = \kappa\rho A, \qquad a_1 = \tfrac{1}{2} c_T (MU^2/D)(1 + D/D_h) + (m - \rho A)g, \qquad a_2 = a_1 e_1 + e_2,$$

$$a_3 = b_1 - a_1,$$

$$e_1 = (1 - \lambda/2)L, \qquad e_2 = \lambda T_0 + \tfrac{1}{2}(1-\lambda)c_b MU^2 + \lambda(1-2\nu)(\bar{p}\bar{A}),$$

$$b_1 = \tfrac{1}{2} c_N (MU^2/D)(1 + D/D_h) + (m - \rho A)g, \qquad a_4 = \tfrac{1}{2} c_N MU/D + \tfrac{1}{2} c_D M/D. \tag{2}$$

In the above, a $(\cdot)$ indicates derivative with respect to time t and $(')$ indicates derivative with respect to x. The upstream and the downstream ends of the cylinder coincide with $x = 0$ and $x = L$ respectively, where boundary conditions may be specified. The various symbols used above are: μ (viscoelastic damping coefficient of cylinder material), E (Young's modulus of the cylinder material), I (moment of inertia of the cylinder cross-section about the centroidal axis), m (mass per unit length of the cylinder), A (cross-sectional area of the cylinder), M (added mass per unit length of the cylinder), κ (coefficient of added mass), D (outer diameter of the cylinder), D_h (hydraulic diameter, $=4A_{ch}/S_{tot}$), A_{ch} (channel flow area when a cluster of cylinders are placed in a channel as in Figure 2a), S_{tot} (total surface area of channel per unit length), L (length of the cylinder), U (constant flow velocity along the cylinder axis), ρ (fluid density), c_N (coefficient of normal drag), c_T (coefficient of tangential drag), c_D (drag coefficient when cylinder is normal to the flow direction), T (tension on the cylinder), c_b (base drag coefficient at the downstream end), g (acceleration due to gravity), p (steady state pressure on the cylinder) and $\bar{p}\bar{A}$ (equals pA at $x = L/2$). The small transverse (y direction) displacement of the cylinder cross-section is denoted $V(x, t)$. The cylinder motion is therefore restricted to the xy-plane. The value of λ is 1 if the downstream end is supported and 0 if free.

Consider equation (1) with $\kappa = 1$ and $h = D/D_h = 0$. This models a single flexible cylinder in laterally unconfined flow. In nuclear fuel bundles, several cylinders are kept close to one another and the entire system is put in a concentric cylindrical flow channel through which flow occurs (see Figure 2). When the stability of a single cylinder in this bundle (cluster) is considered, the added (or hydrodynamic) mass M for this cylinder is

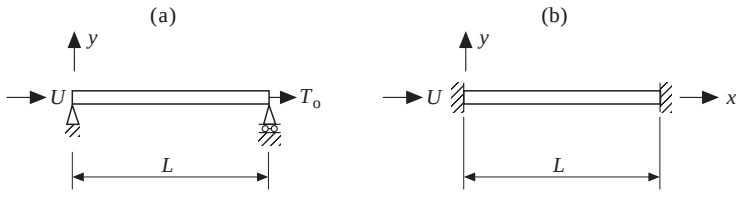

Figure 1. Boundary conditions of cylinders in axial flow: (a) pinned–pinned; (b) clamped–clamped.

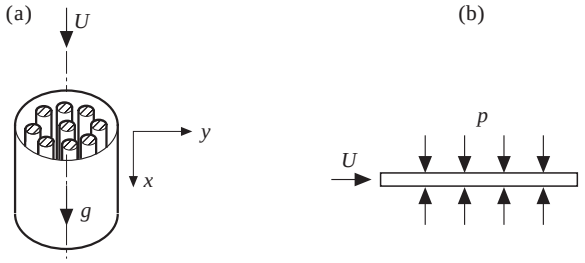

Figure 2. Some additional effects of cylinders in axial flow: (a) Cylinder bundle in axial flow; (b) a cylinder subjected to external pressure.

modified by the coefficient κ. Therefore $\kappa > 1$ represents the case of a single cylinder in a cluster (or bundle) in a confined lateral flow. The effect of lateral confinement is brought out by the finite area of the channel cross-section (A_{ch}) which otherwise is infinite i.e., the cylinder is in an unbounded fluid domain. In nuclear reactor channels and heat exchangers, the bundles are arranged in a vertical direction and hence the self weight effect becomes important and it is given by the second term in the expression for a_1. The lateral forces arising from the mean pressure p of the fluid is given by the third term in the expression for e_2. The frictional forces in the axial and transverse directions of the cylinder are given by the term a_4. In reference [4] as well as in most calculations reported in the literature, it is assumed that $c_N = c_T = c_f$, though c_N and c_T can be different.

It should be noted that equation (1) sets out the problem within the frame work of small amplitude motions (i.e., linear behavior) of the cylinder modelled by elementary (Euler–Bernoulli) beam theory, linearised hydrodynamic force models based on cross-flow principle and a uniform virtual mass of the fluid over the entire length of the cylinder. This theory is valid only when the wave length of vibration of the cylinder is sufficiently large (at least five times) in comparison to the cylinder diameter which allows the "slender body approximation" in the hydrodynamic models. The theory, therefore, rests on twin limitations of linearity in structural behaviour and "slender body approximation" in hydrodynamic behaviour. The fluid effects are accounted for in the structural dynamic equations using certain gross empirical representations, without carrying out any fluid dynamic analysis. This is thus an interaction problem in essence and not in form, and the governing equation of motion is therefore a single equation involving the lateral displacement of the cylinder as the variable.

3. VARIATIONAL FORMULATION

In this section the problem is reduced to a variational form so that finite element approximation can directly follow from it. The solution of equation (1) is assumed in the form

$$V(x, t) = v(x)\, \mathrm{e}^{\mathrm{i}\omega t}, \qquad (i = \sqrt{-1}), \tag{3}$$

where ω is the circular natural frequency of the cylinder. Using equation (3) in equation (1) gives

$$E^*Iv'''' - \omega^2(m + M)v + MU^2v'' + [(a_1 x - a_2)v'' + a_1 v'] + 2\mathrm{i}\omega MUv' + a_3 v' + a_4 \mathrm{i}\omega v = 0, \tag{4}$$

where

$$E^* = E + \mathrm{i}\omega\mu. \tag{5}$$

Multiplying the above equation by a variation δv and integrating over zero to l by parts, (where l is the length of the beam finite element) integration of various term are carried out as follows: first term (by parts integration twice):

$$E^*I \int_0^l (v'')''\delta v \, \mathrm{d}x = E^*I\left\{[(v'')'\delta v - v''\delta v']\Big|_0^l + \delta\left[\int_0^l \tfrac{1}{2} v''^2 \, \mathrm{d}x\right]\right\}; \tag{5a}$$

Second term:

$$\omega^2(m+M) \int_0^l v\delta v \, \mathrm{d}x = \omega^2(m+M)\delta\left[\tfrac{1}{2}\int_0^l v^2 \, \mathrm{d}x\right]; \tag{5b}$$

Third term:

$$MU^2 \int_0^l v''\delta v \, \mathrm{d}x = MU^2\left\{[v'\delta v]\Big|_0^l - \delta\left[\tfrac{1}{2}\int_0^l v'^2 \, \mathrm{d}x\right]\right\}; \tag{5c}$$

Fourth term:

$$\int_0^l (a_1 x - a_2)v''\delta v \, \mathrm{d}x + a_1 \int_0^l v'\delta v \, \mathrm{d}x = [(a_1 x - a_2)v'\delta v]\Big|_0^l - \delta\left[\tfrac{1}{2}\int_0^l (a_1 x - a_2)v'^2 \, \mathrm{d}x\right]. \tag{5d}$$

The fifth and sixth terms yield

$$2MU\mathrm{i}\omega \int_0^l v'\delta v \, \mathrm{d}x, \qquad a_3 \int_0^l v'\delta v \, \mathrm{d}x, \tag{5e}$$

respectively, which remain unaffected.
Seventh term:

$$\mathrm{i}\omega a_4 \int_0^l v\delta v \, \mathrm{d}x = \mathrm{i}\omega a_4 \, \delta\left[\tfrac{1}{2}\int_0^l v^2 \, \mathrm{d}x\right]. \tag{5f}$$

Using equations (5a–f) in equation (4), one obtains the corresponding variational problem as

$$\delta \int_0^l [\tfrac{1}{2} E^*Iv''^2 - \tfrac{1}{2}\omega^2(m+M)v^2 - \tfrac{1}{2} MU^2v'^2 - \tfrac{1}{2}(a_1 x - a_2)v'^2 + \tfrac{1}{2}\mathrm{i}\omega a_4 v^2] \, \mathrm{d}x$$

$$+(2MU\mathrm{i}\omega + a_3)\int_0^l v'\delta v \, \mathrm{d}x = 0, \tag{6}$$

and the corresponding boundary conditions are

$$v = v_0 \text{ or } E^*Iv''' + (MU^2 + a_1 x - a_2)v' = 0 \text{ (at } x = 0, 1) \tag{7}$$

$$v' = 0 \text{ or } E^*Iv'' = 0 \text{ (at } x = 0, 1) \tag{8}$$

4. FINITE ELEMENT APPROXIMATION

The finite element chosen here is the well known two-noded straight uniform beam element with two bending degrees of freedom in the xy-plane at each node. The beam element is shown in Figure 3, and the relevant displacement field and the shape functions are given by [10]:

$$v(x, t) = \sum_{i=1}^{4} N_i(x) u_i(t). \tag{9}$$

$$N_1 = 1 - 3\bar{s}^2 + 2\bar{s}^3; \qquad N_2 = (\bar{s} - 2\bar{s}^2 + \bar{s}^3)l; \qquad N_3 = 3\bar{s}^2 - 2\bar{s}^3;$$
$$N_4 = (-\bar{s}^2 + \bar{s}^3)l; \qquad \bar{s} = x/l \tag{10}$$

where N_j are the standard beam shape functions and u_j are the element degrees of freedom. Using equation (10) in equation (6), one obtains

$$\left[E^*I \int_0^l N_j'' N_i'' \,\mathrm{d}x\right] u_j \,\delta u_i - \left[\omega^2(m + M) \int_0^l N_j N_i \,\mathrm{d}x\right] u_j \,\delta u_i$$
$$- \left[MU^2 \int_0^l N_j' N_i' \,\mathrm{d}x\right] u_j \,\delta u_i - \left[\int_0^l (a_1 x - a_2) N_j' N_i' \,\mathrm{d}x\right] u_j \,\delta u_i$$
$$- \left[i\omega a_4 \int_0^l N_j N_i \,\mathrm{d}x\right] u_j \,\delta u_i + \left[(2MU i\omega + a_3) \int_0^l N_j' N_i \,\mathrm{d}x\right] u_j \,\delta u_i = 0. \tag{11}$$

Noting that δu_i is arbitrary, this equation reduces to the form

$$[-\omega^2[\mathbf{m}_e] + i\omega[\mathbf{c}_e] + [\mathbf{k}_e]]\{\mathbf{u}_j\} = \{\mathbf{0}\}, \qquad (j = 1, 2, 3, 4), \tag{12}$$

where

$$[\mathbf{m}_e] = \sum_{j=1}^{2} m^{(j)}, \qquad [\mathbf{c}_e] = \sum_{j=1}^{3} c^{(j)}, \qquad [\mathbf{k}_e] = \sum_{j=1}^{4} k^{(j)}, \qquad m_{ij}^{(1)} = m \int_0^l N_i N_j \,\mathrm{d}x,$$

$$m_{ij}^{(2)} = M \int_0^l N_i N_j \,\mathrm{d}x, \qquad \mathbf{c}_{ij}^{(1)} = 2MU \int_0^l N_j' N_i \,\mathrm{d}x, \qquad \mathbf{c}_{ij}^{(2)} = a_4 \int_0^l N_i N_j \,\mathrm{d}x,$$

$$\mathbf{c}_{ij}^{(3)} = \mu I \int_0^l N_i'' N_j'' \,\mathrm{d}x, \qquad \mathbf{k}_{ij}^{(1)} = EI \int_0^l N_i'' N_j'' \,\mathrm{d}x, \qquad \mathbf{k}_{ij}^{(2)} = -MU^2 \int_0^l N_i' N_j' \,\mathrm{d}x,$$

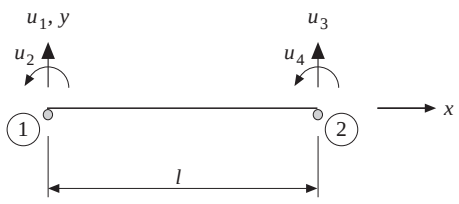

Figure 3. Two dimensional beam element.

$$\mathbf{k}_{ij}^{(3)} = -\int_0^l (a_1 x - a_2) N_i' N_j' \, \mathrm{d}x, \qquad \mathbf{k}_{ij}^{(4)} = a_3 \int_0^l N_j' N_i \, \mathrm{d}x. \tag{13}$$

The matrices $[\mathbf{m}_e]$, $[\mathbf{c}_e]$ and $[\mathbf{k}_e]$ are the element mass, damping and stiffness matrices respectively. Carrying out the usual finite element transformation and assembly, equation (12) results in

$$[-\omega^2[\mathbf{m}] + \mathrm{i}\omega[\mathbf{c}] + [\mathbf{k}]]\{\mathbf{u}\} = \{\mathbf{0}\} \tag{14}$$

where $[\mathbf{m}]$, $[\mathbf{c}]$ and $[\mathbf{k}]$ are the global mass, damping and stiffness matrices and $\{\mathbf{u}\}$ is the vector of all degrees of freedom in the structure. For the non-trivial solution of equation (14)

$$\det[-\omega^2 m_{ij} + \mathrm{i}\omega c_{ij} + k_{ij}] = 0 \tag{15}$$

which is the complex algebraic eigenvalue problem in ω. In the foregoing, it may be noted that the matrices $\mathbf{c}^{(1)}$ and $\mathbf{k}^{(4)}$ are skew symmetric (with $\mathbf{c}_{ij}^{(1)} = -\mathbf{c}_{ji}^{(1)}$, $\mathbf{k}_{ij}^{(4)} = -\mathbf{k}_{ji}^{(4)}$ for $i \neq j$) since they result from "work done" types of expression not having a variational form. As a result $[\mathbf{c}]$ and $[\mathbf{k}]$ matrices are unsymmetric. It can be readily verified that if ω is a root of equation (15), ω^* is also a root (asterisk denotes complex conjugate).

The two boundary conditions used in this study (with upstream end at $x = 0$ and downstream end at $x = L$) are $v = v'' = 0$ at $x = 0$, L (pinned–pinned, denoted hereafter as p–p) and $v = v' = 0$ at $x = 0$, L (clamped–clamped, denoted hereafter as c–c). At this stage the various non-dimensional parameters are listed below which have been used in the literature to present numerical results. These are:

$$\varepsilon = L/D, \qquad \Omega = [M/(EI)]^{1/2}\omega L^2, \qquad u = [M/(EI)]^{1/2} UL, \qquad \beta = M/(m + M),$$

$$\tau = [EI/(m + M)]^{1/2} t/L^2, \qquad \Gamma = T_0 L^2/(EI), \qquad \gamma = (m - M)gL^3/(EI),$$

$$\Pi = (pA)L^2/(EI) \qquad \alpha = [I/\{E(m + M)\}]^{1/2}\mu/L^2, \qquad c = c_D [M/(EI)]^{1/2}. \tag{16}$$

5. ANALYTICAL METHODS

The analytical methods used in the literature are revisited here in order to study the accuracy and convergence of finite element calculations. This is because one needs accurate results based on analytical methods for comparison whereas almost all the results in the literature are in graphical form. In reassessing the analytical methods, certain minor discrepancies were found which also need to be pointed out. In the literature, two methods are used to solve for system frequencies, namely, beam eigenfunction expansion method (BEEM) and power series method (PSM). The BEEM has been used for p–p and c–c cylinders in axial flow and PSM has been used for clamped–free cylinders in axial flow [3]. The order of the determinantal equation defining the eigenvalue problem by BEEM equals the number of eigenfunctions used whereas in PSM it can be reduced to 2. PSM has not been used in p–p and c–c cases in axial flow for unknown reason, i.e., no reason was found in the literature. Since PSM is a powerful method and shorn of the complications of the various beam eigenfunctions, their characteristic equations and closed form evaluation of various integrals required for expansion coefficients and is similar in approach for all boundary conditions, the details of PSM for p–p and c–c boundary conditions are provided in the Appendix A.

TABLE 1

Frequency comparison for single cylinders (p–p and c–c)

Flow velocity (u)	Frequency (Ω) Analytical	Finite element
(a) c–c cylinder with $\beta = 0{\cdot}1$, $\varepsilon c_f = 1$ (Fig. 4 of Ref. [3])		
2	21·1807 + i0·1572	21·1808 + i0·1572
	60·1897 + i0·1582	60·1923 + i0·1582
	119·3000 + i0·1582	119·3219 + i0·1582
4	17·1274 + i0·3079	17·1277 + i0·3079
	55·5338 + i0·3182	55·5368 + i0·3182
	114·3827 + i0·3174	114·4030 + i0·3174
6	6·3510 + i0·4371	6·3522 + i0·4371
	46·8757 + i0·4879	46·8799 + i0·4879
	105·7249 − i0·4796	105·7482 − i0·4796
(b) p–p cylinder with $\beta = 0{\cdot}1$, $\varepsilon c_f = 1$ (Fig. 3 of Ref. [4])		
2	7·5733 + i0·1567	7·5733 + i0·1567
	37·4675 + i0·1584	37·4683 + i0·1584
	86·8639 + i0·1583	86·8716 + i0·1583
3	2·8316 + i0·2321	2·8316 + i0·2321
	34·8037 + i0·2387	34·8045 + i0·2387
	84·3520 + i0·2380	84·3600 + i0·2380
8	5·0754 + i25·7928	5·0755 + i25·7928
	4·6215 − i24·6454	4·6215 − i24·6454
	49·0626 + i0·6870	49·0780 + i0·6870

6. RESULTS AND DISCUSSIONS

Finite element calculations have been carried out for a few example problems, the results of which are available in the literature using analytical methods. These are either presented in the form of Argand diagrams of the complex dimensionless frequencies (Ω) as a function of dimensionless flow velocity (u) or directly by the critical flow velocities for buckling (u_b) and flutter (u_{c0}). For comparison, these graphical results are not good enough and therefore they have been worked out by an analytical method using PSM as discussed in Appendix A. The critical flow velocities can however be directly compared. For one typical problem, a convergence study of the finite element solution for typical flow velocities is reported. A few examples demonstrating the inclusion of intermediate supports (i.e., multispan cylinders), stepped cylinders and the effect of point mass on stability are also presented for which analytical solutions are not possible. The complex eigenvalues from equation (15) have been obtained by a determinant search procedure.

6.1. SINGLE CYLINDER IN AXIAL FLOW

Two examples of single cylinders, one for c–c and the other for p–p boundary conditions, are worked out from reference [3] and the first three Ω values are compared for a few values of u in Table 1(a and b). The results presented in reference [3] for the c–c boundary condition have been found to be wrong due to an error in one of the eigenfunction expansion coefficients. The coefficient should be given by $c_{rr} = \lambda_r \sigma_r (2 - \lambda_r \sigma_r)$ instead of $c_{rr} = \lambda_r \sigma_r (4 - \lambda r \sigma_r)$ as given in Table 1 of this reference. Hence the corrected results for this case in the context of the formulation used in reference [3] are given in the form of an Argand diagram in Figure 4. From Table 1, it can be seen that the comparison of frequencies between finite element and analytical results is virtually

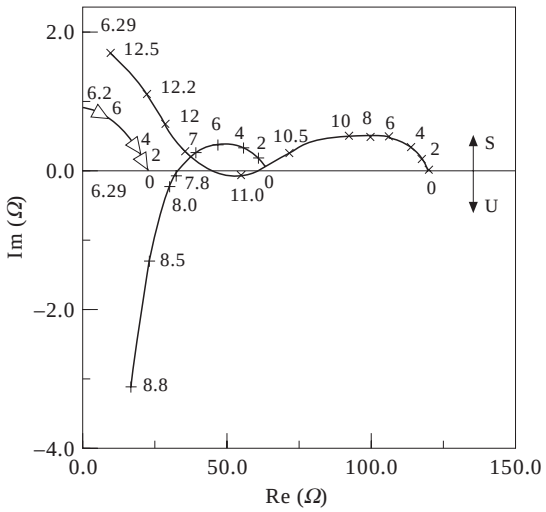

Figure 4. Complex frequency diagram of the lowest three modes of a clamped–clamped cylinder in axial flow for $\beta = 0{\cdot}1$, $\varepsilon c_N = \varepsilon c_T = 1$, $u_{b1} = 6{\cdot}29$, $u_{c0} = 7{\cdot}80$, $11{\cdot}0$. (S, stable, and U, unstable regions). Key: —△—, first mode; —+—, second mode; —×—, third mode.

exact leaving very little to discuss. Similar comparisons have been achieved in all the cases which follow.

6.2. BUNDLE OF CYLINDERS IN AXIAL FLOW

The stability of a p–p and a c-c cylinder in a bundle of cylinders was studied in reference [4] and results were reported in the form of complex frequency diagrams. The u–Ω comparison for the p–p case is presented in Table 2. The critical flow velocities for buckling and flutter for both the cases are compared in Table 4. The results show that instability occurs at much lower flow velocity ($u_{b1} = 1{\cdot}572$ for p–p and $u_{b1} = 3{\cdot}142$ for c–c) in their fundamental mode. For a c–c cylinder, the critical flow velocity for second mode buckling (u_{b2}) was absent.

TABLE 2

Frequency comparison for p–p cylinder in a cluster
$\beta = 0{\cdot}1$, $\varepsilon c_f = 0{\cdot}25$, $h = 1{\cdot}5$, $\kappa = 4$ (Fig. 5 of Ref. [4])

	Frequency (Ω)	
Flow velocity (u)	Analytical	Finite element
0	8·6523 + i0·0	8·6562 + i0·0
	34·6248 + i0·0	34·6247 + i0·0
	77·9059 + i0·0	77·9075 + i0·0
1	6·5892 + i0·01546	6·5892 + i0·01542
	32·9382 + i0·01530	32·9389 + i0·01531
	76·2950 + i0·01526	76·3019 + i0·01524
1·75	0·0 + i4·0817	0·0 + i4·0817
	0·0 − i4·0322	0·0 − i4·0323
	29·2217 + i0·02737	29·2217 + i0·02732
	72·8904 + i0·02699	72·8904 + i0·02695

TABLE 3

Frequency comparison for a p–p cylinder with external tension $\beta = 0{\cdot}1$, $\varepsilon c_f = 0{\cdot}25$, $\Gamma = 10$ (Table 4 of Ref. [4])

Flow velocity (u)	Frequency (Ω)	
	Analytical	Finite element
2	12·4711 + i0·0393	12·4701 + i0·0393
	42·3988 + i0·0396	42·3994 + i0·0396
	91·8296 + i0·0396	91·8368 + i0·0396
4	6·0688 + i0·0763	6·0668 + i0·0763
	36·5375 + i0·0798	36·5383 + i0·0798
	86·0277 + i0·0795	86·0307 + i0·0795
7	0·0 + i13·2720	0·0 + i13·2729
	0·0 − i13·1529	0·0 − i13·1538
	5·4637 + i0·2037	5·4702 + i0·2030
	67·7228 + i0·1430	67·7338 + i0·1431

6.3. EFFECT OF EXTERNALLY APPLIED TENSION

The u–Ω comparison for a p–p cylinder under uniform tension applied externally at the downstream end is given in Table 3. The effect of this parameter (Γ) is to increase the real part of frequency which tends to stabilise the system.

6.4. EFFECT OF SURFACE ROUGHNESS AND PRESSURE DRAG

The effect of surface roughness on the cylinder and pressure drag coefficient is accounted for by the parameters εc_f and εc in equation (2). Table 4 presents the comparison of critical flow velocities for buckling and flutter for a p–p and a c–c cylinder. It is seen from the results that the variations in critical flow velocities are almost nil when compared to the standard case given in the same Table.

TABLE 4

Effect of different parameters on stability by analytical and finite element methods

S. No.	Parameter	Pinned–pinned			Clamped–clamped		
		u_{b1}	u_{b2}	u_{c0}	u_{b1}	u_{b2}	u_{c0}
1	Standard case†	3·143	6·28	6·41	6·29	8·99	9·02
		(3·143)‡	(6·28)	(6·41)	(6·29)	(8·99)	(9·02)
2	$\alpha = 0{\cdot}003$	3·143	6·28	6·52	6·29	9·01	9·20
		(3·143)	(6·28)	(6·56)	(6·28)	(8·99)	(9·21)
3	$\gamma = 10$	3·108	6·30	6·44	6·28	8·99	9·02
		(3·108)	(6·31)	(6·44)	(6·28)	(8·99)	(9·02)
4	$\Pi = 5$,	3·445	6·44	6·55	6·44	9·10	9·12
	$\nu = 0{\cdot}3$	(3·445)	(6·44)	(6·55)	(6·44)	(9·05)	(9·11)
5	$D/D_h = h = 1{\cdot}5$	1·572	3·142	3·143	3·142	–	4·50
	$\kappa = 4$	(1·572)	(3·142)	(3·143)	(3·142)	–	(4·51)
6	$\varepsilon c_f = 1$	3·137	6·31	6·48	6·28	8·98	9·10
		(3·137)	(6·31)	(6·48)	(6·28)	(8·98)	(9·10)
7	$\varepsilon c = 0{\cdot}25$	3·143	6·28	6·41	6·29	8·99	9·02
		(3·143)	(6·28)	(6·41)	(6·29)	(8·99)	(9·05)
8	$\lambda = 0$	3·246	6·49	6·60	6·49	9·28	9·30
		(3·246)	(6·49)	(6·60)	(6·49)	(9·28)	(9·30)

†Standard case here refers to $\beta = 0{\cdot}1$, $\varepsilon c_f = 0{\cdot}25$, $\lambda = \kappa = 1$ [4].
‡Finite element results are given in parenthesis.

6.5. EFFECT OF VISCOELASTIC PROPERTY OF CYLINDER MATERIAL

In reference [4] the Kelvin–Voigt model has been used to represent the internal dissipative forces of cylinder by the parameter α. The effect of this parameter on critical flow velocity (both by analytical and finite element methods) is presented in Table 4 which shows that the critical flow velocity for flutter increases nearly by 2% in both p–p and c–c cases.

6.6. EFFECT OF SELF WEIGHT

The critical flow velocities for buckling and flutter have been obtained by including the effect of gravity parameter (γ), which is relevant when the cylinder is kept in the vertical configuration. The comparison is shown in Table 4. The c–c cylinder does not show any change in critical flow velocity but the p–p cylinder shows a marginal change in its fundamental mode of buckling.

6.7. EFFECT OF EXTERNAL PRESSURISATION

The critical flow velocities are compared for both p–p and c–c cases in Table 4 when the cylinder is externally pressurised by a value given by Π (also see Figure 2b). It can be seen that the critical flow velocity for buckling in fundamental mode has increased by 9% and 3% respectively for these boundary conditions.

6.8. EFFECT OF INTERMEDIATE SUPPORTS

The lowest three non-dimensional complex eigenfrequencies as a function of flow velocity of a uniform circular cylinder for $\beta = 0{\cdot}1$ and $\varepsilon c_f = 1$ with two and three spans are traced as Argand diagrams in Figures 5 and 6 respectively. The critical flow velocity values are presented in Table 5. It is seen from Figure 5 that the loci of the first mode bifurcate on the Im (Ω) axis and with increase of flow velocity the fundamental mode crosses the origin at a critical flow velocity $u_{b1} = 6{\cdot}26$, which is the threshold of buckling instability. As the flow velocity is further increased, the cylinder undergoes buckling instability again at critical flow velocities $u_{b2} = 9{\cdot}17$ and $u_{b3} = 12{\cdot}43$ in second and third modes respectively. For a marginal increase in flow velocity, the dynamic instability occurs as a coupled mode flutter at $u_{c0} = 12{\cdot}59$. It is clearly seen from Figure 6 that with an

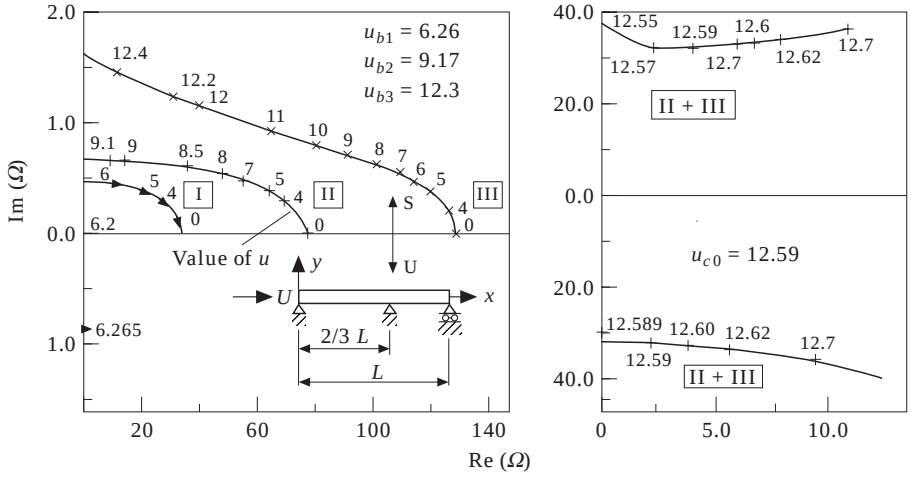

Figure 5. Complex frequency diagram of the lowest three modes of a two span cylinder in axial flow for $\beta = 0{\cdot}1$, $\varepsilon c_f = 1$, $\lambda = \kappa = 1$. Key: —▷—, first mode; —+—, second mode; —×—, third mode.

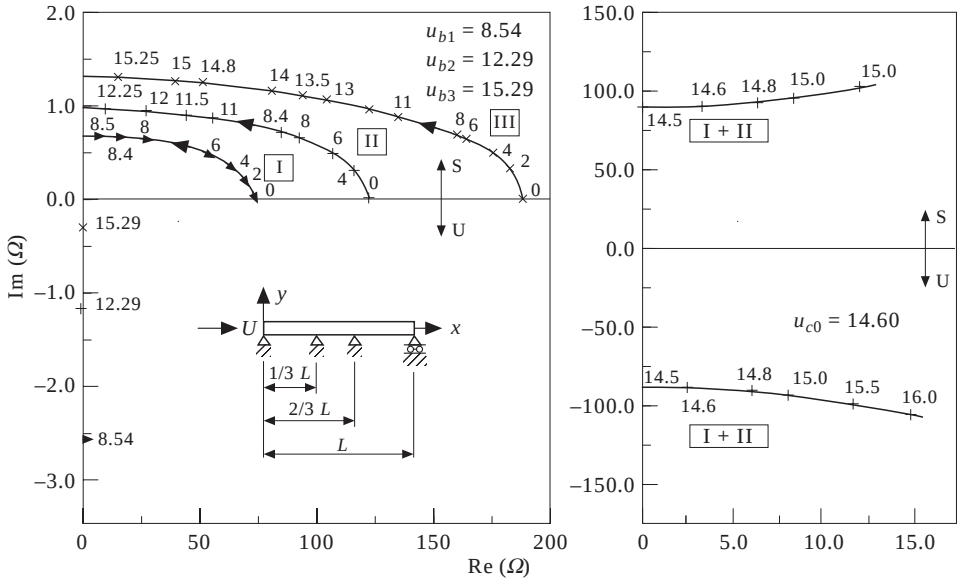

Figure 6. Complex frequency diagram of the lowest three modes of a three span cylinder in axial flow for $\beta = 0{\cdot}1$, $\varepsilon c_f = 1$, $\lambda = \kappa = 1$. Key as for Figure 5.

increase in the number of spans, the critical flow velocity also increases and in this case the coupled mode flutter occurs at $u_{c0} = 14{\cdot}6$ prior to third mode buckling. The fundamental mode of buckling of a two span cylinder occurs at a critical flow velocity which is 100% more than the corresponding single span case for p–p cylinder and 43% more for c–c cylinder. The corresponding values for a three span cylinder are 172% and 57% respectively.

6.9. EFFECT OF STEPPED CYLINDERS

Here a few examples of stepped circular cylinders in uniform axial flow have been examined under the basic assumption that the joints between each segments are smooth so that there is no flow separation at the joints. The dimensional critical flow velocities for the lowest three modes are presented in Table 6. It is seen that for a single stepped cylinder the critical flow velocity for flutter increases from 6·48 m/s to 7·04 m/s, in spite of the fact that the critical flow velocity for buckling has decreased from 3·137 m/s to

TABLE 5

Effect of intermediate supports on stability

S. No.	Configuration	u_{b1}	u_{b2}	u_{c0}	u_{b3}
	$\beta = 0{\cdot}1$, $\varepsilon c_f = 1$, p–p				
1	1 span; (L); (p–p)	3·137	6·31	6·48	9·46
2	2 spans; (2L/3, L/3); (p–p–p)	6·265	9·17	12·59	12·43
3	3 spans; (L/3, L/3, L/3); (p–p–p–p)	8·540	12·29	14·60	15·29
	$\beta = 0{\cdot}1$, $\varepsilon c_f = 1$, c–c				
1	1 span; (L); (c–c)	6·280	8·98	9·10	12·59
2	2 spans; (L/2, L/2); (c–p–c)	8·950	12·59	18·20	15·45
3	3 spans; (L/4, L/4, L/2); (c–p–p–c)	9·880	14·29	14·46	18·47

TABLE 6

Stability of stepped cylinders ($\beta = 0{\cdot}1$, $\varepsilon c_f = 1$, $\lambda = \kappa = 1$)

S. No.	εc_f	Configurations	U_{b1} (m/s)	U_{b2} (m/s)	U_{c0} (m/s)
1 (a)	1	No step; (L, D)	3·137	6·31	6·48
(b)	0·25		3·143	6·28	6·41
2 (a)	1	1 step, ($3L/4$, D)	2·250	4·43	7·04
(b)	0·25	and ($L/4$, $D/2$)	2·480	4·38	8·09
3 (a)	1	2 steps, ($3L/5$, D),	1·120	3·08	4·48
(b)	0·25	($L/5$, $D/2$) and ($L/5$, $D/4$)	1·185	3·57	5·30

Note: $L = 1$ m, $D = 0{\cdot}05$ m, $E = 6{\cdot}4\text{E} + 06$ N/m^2.

2·25 m/s (less by 28%). For the case of two-stepped cylinder, the lowest critical flow velocity is $U_{b1} = 1{\cdot}12$ m/s.

6.10. EFFECT OF POINT MASS

A case of point mass at the mid-span of a simply supported cylinder in axial flow with $\beta = 0{\cdot}1$, $\varepsilon c_f = 1$ was considered. The critical flow velocities are presented in Table 7. It can be seen that the critical flow velocity for buckling (u_b) remains independent of the magnitude of this mass and the critical flow velocity for flutter (u_{c0}) increases marginally from a value of 6·47 to 6·6 for a point mass equal to 100% of structural mass.

6.11. CONVERGENCE STUDY

The convergence results are presented for only one typical case in Table 8. This and many other studies which have been made [2] yield the following conclusions:

(a) For lower flow velocities, 10 elements are required for accurate results.

(b) For higher flow velocities and for higher modes of practical interest, 16 elements are required.

(c) A two- to four-element model gives reasonably good results for the first two modes.

(d) More elements are required for the c–c case than for other boundary conditions.

In other words, a four-element model can be used for the first two roots, a 10-element model for all roots at lower flow velocities and a 16-element model for all situations that could be of practical interest.

TABLE 7

Effect of point mass on critical flow velocities at midspan of a p–p cylinder ($\beta = 0{\cdot}1$, $\varepsilon c_f = 1$, $\kappa = 1$)

Point mass (% of mL)	u_{b1}	u_{b2}	u_{c0}	u_{b3}
0	3·14	6·31	6·47	9·46
25	3·14	6·31	6·47	9·46
50	3·14	6·31	6·47	9·46
75	3·14	6·31	6·48	9·46
100	3·14	6·31	6·60	9·46

TABLE 8

Convergence study of finite element solution for a c–c cylinder ($\beta = 0{\cdot}1$, $\varepsilon c_f = 1$)

Method	Frequency (Ω)	
	$u = 2$	$u = 4$
ANL†	21·1807 + i0·1572	17·1274 + i0·3079
	60·1897 + i0·1582	55·5338 + i0·3182
	119·3100 + i0·1582	114·3827 + i0·3174
FE (2)‡	21·5361 + i0·1576	17·4903 + i0·3121
	80·7184 + i0·1585	76·8141 + i0·3203
FE (4)	21·2134 + i0·1572	17·1812 + i0·3081
	60·7759 + i0·1583	56·1797 + i0·3186
	121·8981 + i0·1583	117·0189 + i0·3184
FE (8)	21·1828 + i0·1572	17·1311 + i0·3079
	60·2303 + i0·1582	55·5805 + i0·3182
	119·5953 + i0·1582	114·6945 + i0·3174
FE (16)	21·1808 + i0·1572	17·1277 + i0·3074
	60·1923 + i0·1582	55·5368 + i0·3182
	119·3219 + i0·1582	114·4030 + i0·3174

†ANL, Analytical.
‡FE, Finite element, number of elements are shown within parenthesis.

7. CONCLUSION

A finite element formulation of the problem of stability of flexible cylinders in axial flow is presented in this work. The complex eigenfrequencies obtained have been validated for a range of examples by comparing them with those obtained from analytical methods. The analytical and finite element results (both eigenfrequencies and critical flow velocities) are in excellent agreement in all cases including those with additional effects. The convergence study indicated that a 16 element model for a cylinder could be used for all results presented in the literature.

The efficacy of the finite element method has been demonstrated using some examples for which analytical methods are either not available or cumbersome to apply. These include two and three span cylinders, stepped cylinders and p–p cylinder with point mass at mid span. The use of multiple supports for a cylinder in axial flow has been found to increase the fundamental critical flow velocity for buckling. On the other hand, the critical flow velocity for a stepped cylinder decreases with reduction in cross-section. The effect of point mass as a percentage variation of structural mass at the midspan of a p–p cylinder reveals firstly that the critical flow velocity for buckling is independent of the magnitude of point mass, since it is a static phenomenon and secondly the critical flow velocity for flutter has increased marginally by 2% for an increase in 100% of structural mass.

The finite element method reported in this work cannot treat the problem of towed–free as well as cantilevered cylinders because in these cases the shape of the end (tapered or blunt) plays a significant role in its stability characteristics. The end effects lead to certain terms in the finite element equations as well as non-conservative follower forces, if any. A more general variational framework based on Hamilton's principle will be required to develop the finite element approximation. The present method can however be readily extended to forced excitation calculations using a direct integration approach. Non-linear structural formulation, to date not studied in the context of the present problem in the literature, can readily be incorporated in any direct integration scheme based upon updated Lagrangian formulation.

REFERENCES

1. S. S. Chen 1988 *Flow-Induced Vibration of Circular Cylindrical Structures*. New York: Hemisphere Publishing Corporation.
2. K. Sudarsan 1996 *PhD Thesis*, *IIT Madras*. Finite element analysis and experimental studies of hydroelastic instability of underwater towed cylindrical structures.
3. M. P. Païdoussis 1966 *Journal of Fluid Mechanics* **26**, 717–736. Dynamics of flexible slender cylinders in axial flow.
4. M. P. Païdoussis 1973 *Journal of Sound and Vibration* **29**, 365–385. Dynamics of cylindrical structures subjected to axial flow.
5. M. P. Païdoussis and S. Suss 1977 *Journal of Applied Mechanics* **44**, 401–407. Stability of a cluster of flexible cylinders in bounded axial flow.
6. G. S. Triantafyllou and C. Chryssostomidis 1985 *American Society of Mechanical Engineers Journal of Energy Resources of Technology* **107**, 421–425. Stability of a string in axial flow.
7. G. S. Triantafyllou and C. Chryssostomidis 1984 *American Society of Mechanical Engineers Journal of Energy Resources Technology* **106**, 246–249. Analytical determination of the buckling speed of towed slender cylindrical beams.
8. M. J. Lighthill 1960 *Journal of Fluid Mechanics* **9**, 305–317. Note on swimming of slender fish.
9. G. I. Taylor 1952 *Proceedings of Royal Society London* **A-214**, 158–183. Analysis of swimming of long and narrow animals.
10. T. Y. Yang 1986 *Finite Element Structural analysis*. NJ: Prentice-Hall.

APPENDIX A: POWER SERIES METHOD

Adopting the notations of reference [3], the non-dimensional differential equation in space cordinates $\xi[Y = Y(\xi)]$ is written as

$$Y'''' + aY'' + cY' + eY = 0 (0 < \xi < 1) \tag{A1}$$

where a, b, c and e are constant coefficients and $Y' = \mathrm{d}Y/\mathrm{d}\xi$ etc. Boundary conditions are:

$$\text{pinned–pinned,} \qquad Y = Y'' = 0, \qquad \text{at} \qquad \xi = 0, 1 \tag{A2}$$

$$\text{clamped–clamped,} \qquad Y = Y' = 0, \qquad \text{at} \qquad \xi = 0, 1 \tag{A3}$$

The solution of (1) is assumed as

$$Y(\xi) = \sum_{n=0}^{\infty} A_n \xi^n. \tag{A4}$$

The various required derivatives are

$$Y' = \sum_{n=0}^{\infty} nA_n \xi^{n-1}, \qquad Y'' = \sum_{n=0}^{\infty} n(n-1)A_n \xi^{n-2}, \qquad Y''' = \sum_{n=0}^{\infty} n(n-1)(n-2)A_n \xi^{n-3}. \tag{A5}$$

Use of equations (A2)–(A4) gives

$$\text{pinned–pinned,} \qquad A_0 = A_2 = A_1 + A_3 + \sum_{n=4}^{\infty} A_n = 6A_3 + \sum_{n=4}^{\infty} n(n-1)A_n = 0, \tag{A6}$$

$$\text{clamped–clamped,} \qquad A_0 = A_1 = A_2 + A_3 + \sum_{n=4}^{\infty} A_n = 2A_2 + 3A_3 + \sum_{n=4}^{\infty} nA_n = 0. \tag{A7}$$

Substituting equation (A4) into equation (A1) and collecting terms of like powers of x, one obtains

$$n(n-1)(n-2)(n-3)A_n + a(n-2)(n-3)A_{n-2} + [b(n-3)(n-4) + c(n-3)]A_{n-3} + eA_{n-4} = 0. \tag{A8}$$

One writes this relation as

$$A_n = f_{1n} A_{n-2} + f_{2n} A_{n-3} + f_{3n} A_{n-4}, \tag{A9a}$$

where

$$f_{1n} = -a/n(n-1), \qquad f_{2n} = -[b(n-3)(n-4) + c(n-3)]/n(n-1)(n-2)(n-3),$$
$$f_{3n} = -e/n(n-1)(n-2)(n-3) \tag{A9b–d}$$

In view of equation (A8), one obtains for various cases

$$\text{pinned–pinned}, \qquad A_n = G_n A_1 + H_n A_3, \tag{A10a}$$

$$\text{clamped–clamped}, \qquad A_n = G_n A_2 + H_n A_3, \tag{A10b}$$

where for the *pinned–pinned* case up to $n = 3$

$$G_1 = H_3 = 1, \qquad H_1 = H_2 = G_2 = G_3 = 0, \tag{A11a}$$

and for the *clamped–clamped* case up to $n = 3$

$$G_2 = H_3 = 1, \qquad G_1 = H_1 = H_2 = G_3 = 0. \tag{A11b}$$

Using (A10a) or (A10b) in (A9) one obtains

$$G_n = f_{1n} G_{n-2} + f_{2n} G_{n-3} + f_{3n} G_{n-4}, \qquad H_n = f_{1n} H_{n-2} + f_{2n} H_{n-3} + f_{3n} H_{n-4}. \tag{A12a, b}$$

Using these recursive relations in equation (A6), (A7) and (A11) in conjunction with either equations (A10a) or (A10b), one obtains a system of equations

$$[\mathbf{a}_{ij}]\{\mathbf{B}_j\} = \{\mathbf{0}\} \tag{A13}$$

where for a *pinned–pinned* cylinder

$$B_1 = A_1, \qquad B_2 = A_3, \qquad a_{11} = 1 + \sum_{n=4}^{\infty} G_n, \qquad a_{12} = 1 + \sum_{n=4}^{\infty} H_n,$$

$$a_{21} = \sum_{n=4}^{\infty} n(n-1)G_n, \qquad a_{22} = 6 + \sum_{n=4}^{\infty} n(n-1)H_n, \tag{A14a}$$

and for a *clamped–clamped* cylinder

$$B_1 = A_2, \qquad B_2 = A_3, \qquad a_{11} = 1 + \sum_{n=4}^{\infty} G_n, \qquad a_{12} = 1 + \sum_{n=4}^{\infty} H_n,$$

$$a_{21} = 2 + \sum_{n=4}^{\infty} G_n, \qquad a_{22} = 3 + \sum_{n=4}^{\infty} nH_n. \tag{A14b}$$

For non-trivial solutions one requires

$$f(\Omega) = |a_{ij}| = 0. \tag{A15}$$